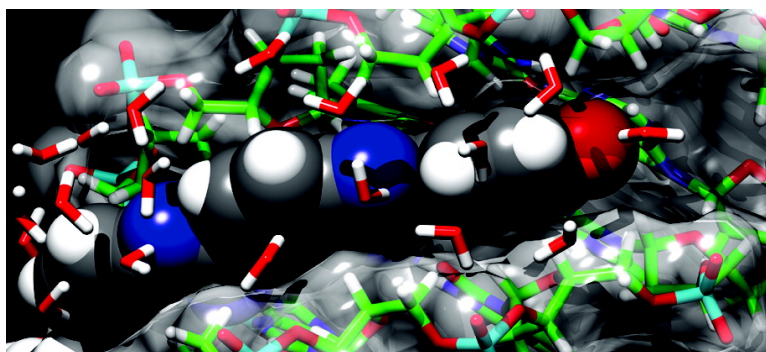


## The Dynamics of Water at DNA Interfaces: Computational Studies of Hoechst 33258 Bound to DNA

Kristina E. Furse, and Steven A. Corcelli

*J. Am. Chem. Soc.*, **2008**, 130 (39), 13103-13109 • DOI: 10.1021/ja803728g • Publication Date (Web): 04 September 2008

Downloaded from <http://pubs.acs.org> on February 8, 2009



### More About This Article

Additional resources and features associated with this article are available within the HTML version:

- Supporting Information
- Links to the 1 articles that cite this article, as of the time of this article download
- Access to high resolution figures
- Links to articles and content related to this article
- Copyright permission to reproduce figures and/or text from this article

[View the Full Text HTML](#)

## The Dynamics of Water at DNA Interfaces: Computational Studies of Hoechst 33258 Bound to DNA

Kristina E. Furse and Steven A. Corcelli\*

*Department of Chemistry and Biochemistry, University of Notre Dame,  
Notre Dame, Indiana 46556*

Received May 19, 2008

**Abstract:** Together, spectroscopy combined with computational studies that relate directly to the experimental measurements have the potential to provide unprecedented insight into the dynamics of important biological processes. Recent time-resolved fluorescence experiments have shown that the time scales for collective reorganization at the interface of proteins and DNA with water are more than an order of magnitude slower than in bulk aqueous solution. The molecular interpretation of this change in the collective response is somewhat controversial — some attribute the slower reorganization to dramatically retarded water motion, while others describe rapid water dynamics combined with a slower biomolecular response. To connect directly to solvation dynamics experiments of the fluorescent probe Hoechst 33258 (H33258) bound to DNA, we have generated 770 ns of molecular dynamics (MD) simulations and calculated the equilibrium and nonequilibrium solvation response to excitation of the probe. The calculated time scales for the solvation response of H33258 free in solution (0.17 and 1.4 ps) and bound to DNA (1.5 and 20 ps) are highly consistent with experiment (0.2 and 1.2 ps, 1.4 and 19 ps, respectively). Decomposition of the calculated response revealed that water solvating the probe bound to DNA was still relatively mobile, only slowing by a factor of 2–3, while DNA motion was responsible for the long-time component (~20 ps).

### I. Introduction

Time-resolved spectroscopy is an extremely useful tool to probe dynamics on ultrafast time scales. Accurate theoretical modeling can provide powerful insight by helping to relate experimental observables to specific microscopic interactions. There is currently great interest in using these methods, which have greatly aided the understanding of bulk solvent dynamics,<sup>1–3</sup> to investigate the behavior of water near biomolecules, sometimes referred to as biological water.<sup>4,5</sup> Time-dependent Stokes shift experiments measure the collective response of the environment to electronic excitation of a fluorescent probe. Using molecular dynamics (MD) simulations, the response can be decomposed into individual contributions from environmental components, including water, ions, and biomolecules. While this decomposition is tremendously interesting, it is difficult to validate because unlike the total response, there is no experimental observable to directly assess the accuracy of the individual component responses. Recent computational studies of solvation dynamics in biological systems have yielded very different decompositions, leading to conflicting interpretations of the behavior of water at biological interfaces.<sup>6–10</sup>

Combining the results from three different experimental techniques spanning different timeframes, Berg and co-workers showed that the Stokes shift for a DNA bound probe increases continuously throughout a 40 fs to 40 ns time range.<sup>11</sup> Associated MD studies identified water as the dominant contributor to the response and anomalous power-law dynamics.<sup>6</sup> Zewail and co-workers experimentally characterized the time frame from 100 fs to 200 ps using ultrafast fluorescence spectroscopy.<sup>12</sup> They observed that the solvation times for the fluorescent probe Hoechst 33258 (H33258) bound to the minor groove of DNA (1.5 and 19 ps) were more than an order of magnitude slower than for the probe free in aqueous solution (0.2 and 1.2 ps), a difference they attributed to a change in the collective reorganization of water molecules at the DNA/water interface. This interpretation was supported by a subsequent MD study by Hynes and co-workers.<sup>10</sup> More recent studies using a fluorescent probe intercalated into DNA also gave dynamic Stokes shift time constants of around 1 and 20 ps.<sup>13</sup> Similar solvation times on the order of 20–40 ps have been observed experimentally for various probes in proteins as well, prompting

- (1) Fleming, G. R.; Cho, M. H. *Annu. Rev. Phys. Chem.* **1996**, *47*, 109–134.
- (2) Jimenez, R.; Fleming, G. R.; Kumar, P. V.; Maroncelli, M. *Nature* **1994**, *369*, 471–473.
- (3) Stratt, R. M.; Maroncelli, M. *J. Phys. Chem.* **1996**, *100*, 12981–12996.
- (4) Raschke, T. M. *Curr. Opin. Struct. Biol.* **2006**, *16*, 152–159.
- (5) Pal, S. K.; Peon, J.; Bagchi, B.; Zewail, A. H. *J. Phys. Chem. B* **2002**, *106*, 12376–12395.
- (6) Berg, M. A.; Coleman, R. S.; Murphy, C. J. *Phys. Chem. Chem. Phys.* **2008**, *10*, 1229–1242.
- (7) Golosov, A. A.; Karplus, M. *J. Phys. Chem. B* **2007**, *111*, 1482–1490.

- (8) Li, T. P.; Hassanali, A. A. P.; Kao, Y. T.; Zhong, D. P.; Singer, S. J. *J. Am. Chem. Soc.* **2007**, *129*, 3376–3382.
- (9) Nilsson, L.; Halle, B. *Proc. Natl. Acad. Sci. USA* **2005**, *102*, 13867–13872.
- (10) Pal, S.; Maiti, P. K.; Bagchi, B.; Hynes, J. T. *J. Phys. Chem. B* **2006**, *110*, 26396–26402.
- (11) Andreatta, D.; Lustres, J. L. P.; Kovalenko, S. A.; Ernsting, N. P.; Murphy, C. J.; Coleman, R. S.; Berg, M. A. *J. Am. Chem. Soc.* **2005**, *127*, 7270–7271.
- (12) Pal, S. K.; Zhao, L. A.; Zewail, A. H. *Proc. Natl. Acad. Sci. USA* **2003**, *100*, 8113–8118.
- (13) Furstenberg, A.; Vauthey, E. *J. Phys. Chem. B* **2007**, *111*, 12610–12620.

the interpretation that water dominates the solvation response, and interaction of the probe with the biomolecule does not make a significant contribution.<sup>5,12,14</sup>

Halle and co-workers challenged these interpretations based on magnetic relaxation dispersion (MRD)<sup>15,16</sup> experiments and MD simulations of the protein monellin.<sup>9</sup> Using a linear response approach, they found that the water response decayed rapidly, and that the protein dynamics accounted for the long-time response. Yet another study by Singer and co-workers demonstrated both types of results in the same simulation: initially, water dominated the slow component of the solvation response, but after a conformational change, the slow component was instead dominated by protein motion.<sup>8</sup> Computational work by Golosov and Karplus shed light on this apparent contradiction by demonstrating that the relative contributions of water and protein to the solvation response depended on the location of the probe.<sup>7</sup> Recent experiments demonstrated that probe location also has a significant effect on the collective solvation response in proteins.<sup>17</sup> So, while multiple proteins and even DNA exhibit solvation responses with similar time scales, the balance of water and biomolecule contributions appears to be highly dependent on the specific nature of the interactions. Taken together, these studies demonstrate the inherent complexity of the solvation response in biological environments. As a result, definitive molecular interpretation of solvation dynamics experiments remains a challenge.

In this work, we have used solvation dynamics calculations to connect directly to the time-resolved fluorescence experiments of Zewail and co-workers<sup>12</sup> to further investigate the dynamics of water at the DNA interface. The H33258/DNA system has been extensively characterized, providing a basis for modeling and validating our simulations. X-ray crystal structures have been reported for the DNA duplex with<sup>18</sup> and without<sup>19</sup> H33258 bound, and the photophysical properties of the probe have been studied in bulk and when bound to DNA.<sup>20,21</sup> We have conducted an extensive investigation using both equilibrium and nonequilibrium approaches on multiple independent trajectories with a detailed model of the H33258 fluorophore. From the simulations, we determined the relative contributions of water, ions, DNA, and solute conformational energy to the collective response, and found that the water response was only 2–3 times slower than that for the unbound probe. Furthermore, the water response was dominated by contributions from the first hydration shell of the probe, which represents a small subset of relatively mobile waters at the DNA interface. The long time-scale response (20 ps) was traced to collective motions of the DNA.

## II. Theoretical and Computational Methods

**A. Solvation Dynamics Calculations.** The response of the environment (water, counterions, and DNA) to electrostatic perturbation of the fluorescent probe H33258 was studied using both equilibrium and nonequilibrium MD simulations (Section II-C). The calculations, based on methodology developed in numerous previous MD studies of solvation dynamics,<sup>7–10,22–24</sup> center on the instantaneous solvation energy,  $\Delta E(t) = E_{\text{excited}}(t) - E_{\text{ground}}(t)$ , which describes the difference in solute–solvent interaction energy with the solute in its ground and excited electronic states. The excitation is modeled classically as a redistribution of solute atomic partial charges.

Our solvation dynamics method differs from previous investigations in two important respects: direct inclusion of the solute intramolecular energy in  $\Delta E(t)$ , and use of the cutoff-neutralized damped shifted force (DSF) sum to account for long-range electrostatic interactions.<sup>25–27</sup> The latter was extensively validated by Fennell and Gezelter,<sup>25</sup> who demonstrated that DSF yields results consistent with more established Ewald-based methods.<sup>28</sup> We validated the protocol for H33258 free in solution, and the method and results are described in detail elsewhere.<sup>29</sup> Briefly, in terms of  $\Delta E$ , the normalized solvation response function,  $S(t)$ , is expressed as

$$S(t) = \frac{\overline{\Delta E(t)} - \langle \Delta E(\infty) \rangle_1}{\langle \Delta E(0) \rangle_0 - \langle \Delta E(\infty) \rangle_1} \quad (1)$$

where the overbar represents an average of independent non-equilibrium trajectories, and  $\langle \dots \rangle_{0(1)}$  denotes an equilibrium average with the solute in its ground and excited states, respectively. Within linear response theory,  $S(t)$  is equal to the equilibrium time correlation function of fluctuations in the solvation energy differences,<sup>22,30</sup>

$$S(t) \cong C_{0(1)}(t) = \frac{\langle \delta \Delta E(0) \delta \Delta E(t) \rangle_{0(1)}}{\langle (\delta \Delta E)^2 \rangle_{0(1)}} \quad (2)$$

where  $\delta \Delta E(t) = \Delta E(t) - \langle \Delta E \rangle_{0(1)}$ , and  $\langle \dots \rangle_{0(1)}$  represents an ensemble average in either the ground or excited state of the solute.  $C_0(t)$  and  $C_1(t)$  presented in this work represent averages for seven independent 15 ns ground and excited-state equilibrium trajectories, respectively.

**B. Decomposition of the Collective Solvation Response.** Because  $\Delta E$  is calculated as a simple pairwise electrostatic sum, it can be decomposed into individual DNA, water, and ion contributions,  $\Delta E = \Delta E^{\text{DNA}} + \Delta E^{\text{water}} + \Delta E^{\text{ion}} + \Delta E^{\text{conf}}$ . The final component,  $\Delta E^{\text{conf}}$ , represents interaction of the solute with itself through electrostatic terms in the solute intramolecular molecular mechanics potential energy. Because we have incorporated full flexibility in our model of the large H33258 probe,  $\Delta E^{\text{conf}}$  varies as the atoms of the solute move relative to one another, contributing to the collective solvation response.

- (14) Pal, S. K.; Peon, J.; Zewail, A. H. *Proc. Natl. Acad. Sci. USA* **2002**, *99*, 15297–15302.  
 (15) Halle, B. In *Hydration Processes in Biology*; Bellisent-Funel, M.-C., Ed.; IOS Press: Dordrecht, The Netherlands, 1998, pp 233–249.  
 (16) Halle, B. *Philos. Trans. R. Soc. London B* **2004**, *359*, 1207–1223.  
 (17) Abbyad, P.; Shi, X. H.; Childs, W.; McAnaney, T. B.; Cohen, B. E.; Boxer, S. G. *J. Phys. Chem. B* **2007**, *111*, 8269–8276.  
 (18) Vega, M. C.; Saez, I. G.; Aymami, J.; Eritja, R.; Vandermarel, G. A.; Vanboom, J. H.; Rich, A.; Coll, M. *Eur. J. Biochem.* **1994**, *222*, 721–726.  
 (19) Edwards, K. J.; Brown, D. G.; Spink, N.; Skelly, J. V.; Neidle, S. J. *Mol. Biol.* **1992**, *226*, 1161–1173.  
 (20) Cosa, G.; Focsaneanu, K. S.; McLean, J. R. N.; McNamee, J. P.; Scaiano, J. C. *Photochem. Photobiol.* **2001**, *73*, 585–599.  
 (21) Kalninsk, K. K.; Pestov, D. V.; Roshchina, Y. K. *J. Photochem. Photobiol., A* **1994**, *83*, 39–47.

- (22) Carter, E. A.; Hynes, J. T. *J. Chem. Phys.* **1991**, *94*, 5961–5979.  
 (23) Ingrosso, F.; Ladanyi, B. M.; Mennucci, B.; Elola, M. D.; Tomasi, J. *J. Phys. Chem. B* **2005**, *109*, 3553–3564.  
 (24) Kumar, P. V.; Maroncelli, M. *J. Chem. Phys.* **1995**, *103*, 3038–3060.  
 (25) Fennell, C. J.; Gezelter, J. D. *J. Chem. Phys.* **2006**, *124*, 234104.  
 (26) Wolf, D.; Koblinski, P.; Phillpot, S. R.; Eggebrecht, J. *J. Chem. Phys.* **1999**, *110*, 8254–8282.  
 (27) Zahn, D.; Schilling, B.; Kast, S. M. *J. Phys. Chem. B* **2002**, *106*, 10725–10732.  
 (28) Darden, T.; York, D.; Pedersen, L. *J. Chem. Phys.* **1993**, *98*, 10089–10092.  
 (29) Furse, K. E.; Lindquist, B. A.; Corcelli, S. A. *J. Phys. Chem. B* **2008**, *112*, 3231–3239.  
 (30) Laird, B. B.; Thompson, W. H. *J. Chem. Phys.* **2007**, *126*, 211104.

Normalized component solvent response functions,  $S\alpha(t)$ , were calculated from the individual components of  $\Delta E$ ,

$$S^\alpha(t) = \frac{\overline{\Delta E^\alpha(t)} - \langle \Delta E^\alpha(\infty) \rangle_1}{\langle \Delta E(0) \rangle_0 - \langle \Delta E(\infty) \rangle_1} \quad (3)$$

where the superscript  $\alpha$  indicates the component of interest (water, ion, DNA, or solute conformation). Unlike the straightforward decomposition of  $S(t)$ , there are multiple ways to divide  $C(t)$  into components. While cross- and autocorrelations of the components of  $\Delta E$  can reveal interesting information about interactions in the system, reduced partial time correlation functions yield  $C\alpha(t)$  that are rigorously analogous to the normalized component  $S\alpha(t)$  response functions.<sup>7,9,31</sup>

$$C_{0(1)}^\alpha(t) = \frac{\langle \Delta E^\alpha(t) \Delta E(0) \rangle_{0(1)} - \langle \Delta E^\alpha \rangle_{0(1)} \langle \Delta E \rangle_{0(1)}}{\langle \Delta E(0) \Delta E(0) \rangle_{0(1)} - \langle \Delta E \rangle_{0(1)} \langle \Delta E \rangle_{0(1)}} \quad (4)$$

**C. Molecular Dynamics Setup and Simulation.** MD simulations of the DNA/H33258 complex were performed using *AMBER 9.0*<sup>32</sup> with the *AMBER ff99* force field<sup>33</sup> and the *SPC/E* water model.<sup>34</sup> The development of molecular mechanics force field parameters for ground and excited state H33258 is described in detail elsewhere.<sup>29</sup> The X-ray crystal structure of H33258 bound to the minor groove of the A-tract DNA dodecamer d(CGCAAATTTGCG),<sup>18</sup> including crystallographic water molecules, was solvated in a cubic periodic box, with a minimum buffer of 10 Å between any DNA or solute atom and the closest box edge. Sodium counterions were added to establish charge neutrality. The resulting 27 415 atom system, consisting of the DNA, H33258, 21 Na<sup>+</sup>, and 8859 water molecules (Figure 1) was subjected to a 1.2 ns equilibration procedure similar to that described for the unbound probe.<sup>29</sup> Complete simulation details are included as Supporting Information.

Seven independent ground-state production MD trajectories were performed in the NVE ensemble with the H33258/DNA complex fully flexible, except all covalent bonds containing hydrogen were fixed at equilibrium lengths using the SHAKE algorithm.<sup>35</sup> A 2 fs integration time step was used and configurations were collected every 10 fs for the first 2 ns, and every 100 fs thereafter. A particle-mesh Ewald summation method was used to compute long-range electrostatic interactions,<sup>28</sup> with a 9 Å real-space nonbonded cutoff. The data collection phase for each of the seven trajectories was 15 ns, for a total of 105 ns of ground-state equilibrium simulation data at 100 fs temporal resolution (14 ns at 10 fs resolution).

Independent snapshots taken every 10 ps from the first 8 ns of all seven ground-state trajectories (5600 total) were used as initial configurations for the nonequilibrium trajectories. The ground-state solute parameters were instantaneously replaced with the excited-state parameters, and each of the 5600 trajectories was extended to 100 ps. Configurations were collected every 10 fs for the first 5 ps, and every 100 fs thereafter. Seven of the nonequilibrium trajectories were

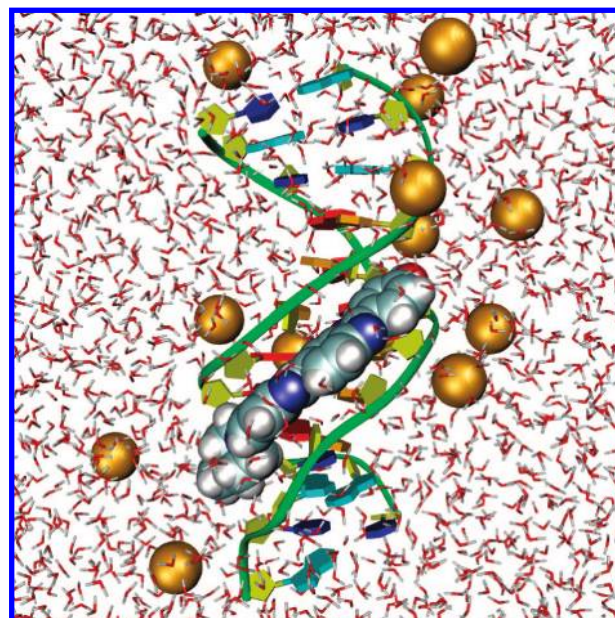


**Figure 1.** The MD simulation system consisted of the probe H33258 bound to the dodecamer d(CGCAAATTTGCG) in a periodic box of water and sodium counterions (orange spheres). For clarity, most of the water and some ions have been omitted. The probe is colored by element: C (gray), O (red), N (blue), and H (white). The DNA is colored by substructure, with A (red), T (orange), G (cyan), C (blue), and the sugar–phosphate backbone represented by green ribbon connecting yellow deoxyribose rings.

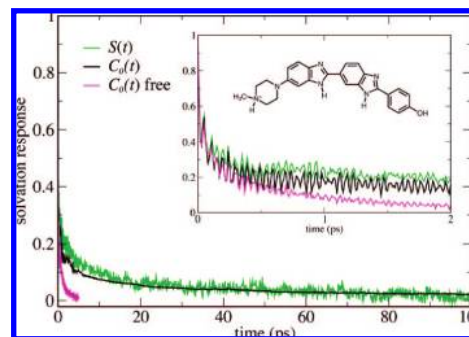


**Figure 2.** Nonequilibrium solvation response,  $S(t)$  (green), and ground-state equilibrium correlation functions,  $C_0(t)$ , calculated for the fluorescent probe H33258 bound to DNA (black) and free in aqueous solution (magenta). Expansion of the first two picoseconds of the response at 10-fold higher temporal resolution (10 fs) reveals reproducible oscillations associated with probe flexibility (inset). The chemical structure of H33258 is also shown.

extended further for a total of 105 ns of excited-state equilibrium simulation data at 100 fs temporal resolution.

### III. Results and Discussion

**A. Total Solvation Response.** We calculated the nonequilibrium solvation response,  $S(t)$ , and ground and excited-state equilibrium correlation functions,  $C_0(t)$  and  $C_1(t)$ , for simulations of H33258 bound to DNA (Figure 2), and fit the results to a triexponential function to extract time scales (equation in Table 1). While multiexponential models are commonly used to fit solvation response data in simple solvents, the nature of the most appropriate fit function for biological systems is a matter of debate. The longer time scale values are sensitive to fitting conditions, including the selected time range, and multiexponentials have proven inappropriate to describe the increasingly

(31) Bernard, W.; Callen, H. B. *Rev. Mod. Phys.* **1959**, *31*, 1017–1044.

(32) Case, D. A.; et al. *AMBER 9*; University of California: San Francisco, 2006.

(33) Wang, J. M.; Cieplak, P.; Kollman, P. A. *J. Comput. Chem.* **2000**, *21*, 1049–1074.

(34) Berendsen, H. J. C.; Grigera, J. R.; Straatsma, T. P. *J. Phys. Chem.* **1987**, *91*, 6269–6271.

(35) Ryckaert, J. P.; Ciccotti, G.; Berendsen, H. J. C. *J. Comput. Phys.* **1977**, *23*, 327–341.

**Table 1.** Time Constants and Amplitudes of Multiexponential Fits<sup>a</sup> to the Experimental and Calculated Solvation Response and Equilibrium Correlation Functions

		$a_1$ (%)	$\tau_1$ (fs)	$a_2$ (%)	$\tau_2$ (ps)	$a_3$ (%)	$\tau_3$ (ps)	$a_4$ (%)
free probe	$C_0(t)$	52	$9.5 \pm 0.6^b$	30	$0.17 \pm 0.01$	18	$1.36 \pm 0.04$	
	$C_1(t)$	53	$9.4 \pm 0.6$	30	$0.18 \pm 0.01$	17	$1.39 \pm 0.04$	
	$S(t)$	51	$9 \pm 3$	30	$0.16 \pm 0.04$	19	$1.4 \pm 0.2$	
	Expt <sup>c</sup>			33	0.20	67	1.2	
DNA/probe	$C_0(t)$	71	$47 \pm 3$	18	$1.37 \pm 0.08$	8.7	$20.5 \pm 0.9$	2.3
	$C_1(t)$	70	$61 \pm 4$	18	$1.83 \pm 0.15$	9.7	$18.9 \pm 1.2$	2.3
	$S(t)$	70	$24 \pm 2$	18	$2.6 \pm 0.3$	10	$30 \pm 7$	1.4
	Expt <sup>c</sup>			64	1.4	36	19	

<sup>a</sup>  $y = a_1 \exp(-t/\tau_1) + a_2 \exp(-t/\tau_2) + a_3 \exp(-t/\tau_3) + a_4$ , where  $a_1 + a_2 + a_3 + a_4 = 1$ . <sup>b</sup> Time constants reported with 95% confidence intervals. <sup>c</sup> Ref 12.

**Table 2.** Time Constants for the Isolated Water Component

		$\tau_{>}$ (ps)	$\tau_3$ (ps)
free probe	$C_0^{\text{water}}(t)$	$0.176 \pm 0.006$	$1.31 \pm 0.02$
	$C_1^{\text{water}}(t)$	$0.170 \pm 0.008$	$1.29 \pm 0.02$
DNA/probe	$C_0^{\text{water}}(t)$	$0.4 \pm 0.1$	$2.7 \pm 0.3$
	$C_1^{\text{water}}(t)$	$0.7 \pm 0.2$	$4.5 \pm 0.6$

large range of relaxation times observed in proteins and DNA.<sup>6,17</sup> Berg and co-workers have even questioned the validity of extracting unique times from the broad relaxation range they have observed for aqueous DNA.<sup>6</sup> For the present work, triexponential fits are well suited to the relatively small 10 fs to 100 ps time range (Supporting Information) and were chosen to facilitate comparison to the time-dependent Stokes shift experiments of Zewail and co-workers<sup>12</sup> to validate our calculations. Our results are shown in Table 1 along with the experimental results and our control simulations of H33258 in aqueous solution.<sup>29</sup> The 95% confidence intervals given in Table 1 describe the scatter of data points around the fit curves and therefore should be interpreted as a lower estimate of error that does not include any potential systematic error resulting from the choice of model and time interval for the fits (Supporting Information).

All of the computational response functions include a well-documented ultrafast inertial relaxation ( $\tau_1$ ) that is beyond the experimental resolution of  $\sim 100$  fs. This inertial response has been shown to account for approximately 50% of the total solvation response in aqueous solution on a time scale of  $\sim 20$  fs.<sup>2,24</sup> In this work, we captured the ultrafast response in  $\tau_1$  by using a triexponential fit for both the free probe and the DNA-bound probe. We note that similar free probe simulations are often fit with a biexponential function.<sup>9,23</sup> A biexponential fit of our free probe data from the 0–5 ps time range gives  $\tau_1 = 22$  fs,  $a_1 = 71\%$ ;  $\tau_2 = 0.87$  ps,  $a_2 = 29\%$ , but  $\chi^2$  is twice as large (Supporting Information). We also note that the values of  $\tau_1$  for the collective solvation response reported in Table 1 do not correspond directly to known inertial water dynamics. In our solution phase calculations,  $\tau_1$  appears faster than expected (9 fs) due to the inclusion of solute conformational relaxation in the instantaneous solvation energy,  $\Delta E(t)$  ( $\tau_1 = 20$  fs,  $a_1 = 45\%$  for the isolated water component). It appears slower (50–60 fs) in  $C(t)$  for the DNA-bound probe due to the 10-fold lower temporal resolution (100 fs) in our equilibrium DNA/probe simulations ( $\tau_1 = 25$  fs,  $a_1 = 53\%$  for the isolated water component from 10 fs resolution simulations).

Our calculated noninertial time scales,  $\tau_2$  and  $\tau_3$ , which relate to diffusive motions in water, are highly consistent with the experimental results. The 10-fold increases in  $\tau_2$  and  $\tau_3$  when the probe binds to DNA are duplicated in the equilibrium correlation functions,  $C(t)$ , and slightly overestimated in the

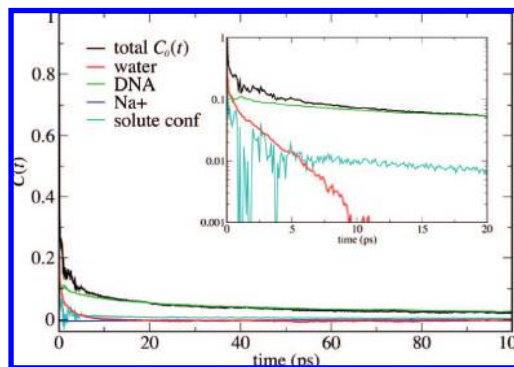


**Figure 3.** Decomposition of the ground-state equilibrium correlation function,  $C_0(t)$ , into individual contributions from water, DNA, sodium counterions, and solute conformation. DNA is primarily responsible for the long-time components of the collective response, while the water response decays rapidly. The inset shows a semilog plot of the first 20 ps.

nonequilibrium solvation response,  $S(t)$ . Although  $S(t)$  is more directly related to time-dependent fluorescence experiments (eq 1), it requires an enormous amount of sampling to achieve good statistics for quantitative analysis.  $S(t)$  for the DNA-bound probe is based on 560 ns of nonequilibrium simulations to calculate  $\Delta E(t)$ , plus 210 ns of ground and excited-state equilibrium simulations to estimate  $\Delta E(0)$  and  $\Delta E(\infty)$ , yet it still exhibits a significant amount of statistical noise (Figure 2) that leads to greater uncertainty in the fits (Table 1). In contrast,  $C(t)$  has vastly superior statistics (Table 1). While significant deviation from linear response behavior is not expected for relatively subtle charge redistributions in large chromophores like H33258,  $S(t)$  is extremely valuable for independent verification of the results, especially the component decomposition for which there is no direct experimental basis for comparison.

One notable difference between the calculated and experimental responses for the probe bound to DNA is the presence of a small constant offset (1–2% of the total decay) in the fits of both  $C(t)$  and  $S(t)$  (Table 1). When the time interval for the correlation functions is extended (from 0–100 ps to 0–350 ps), the long-term correlation is well fit by a fourth exponential with time constants of 200 and 250 ps for  $C_0(t)$  and  $C_1(t)$ , respectively. Hynes and co-workers noticed a very similar slow component ( $\sim 250$  ps) in solvation dynamics calculations for a DNA simulation of similar length (15 ns, 1 ps temporal resolution).<sup>10</sup> Ultimately, extremely long simulations, in the 100 ns to  $\mu$ s range, with more realistic ionic environments may be needed to accurately model the entire range of reorganization time scales at the DNA interface seen in experiment.<sup>11</sup>

**B. Component-Based Decomposition.** The strong agreement between our theoretical results and the experimental solvation responses validates our methodology and suggests that the

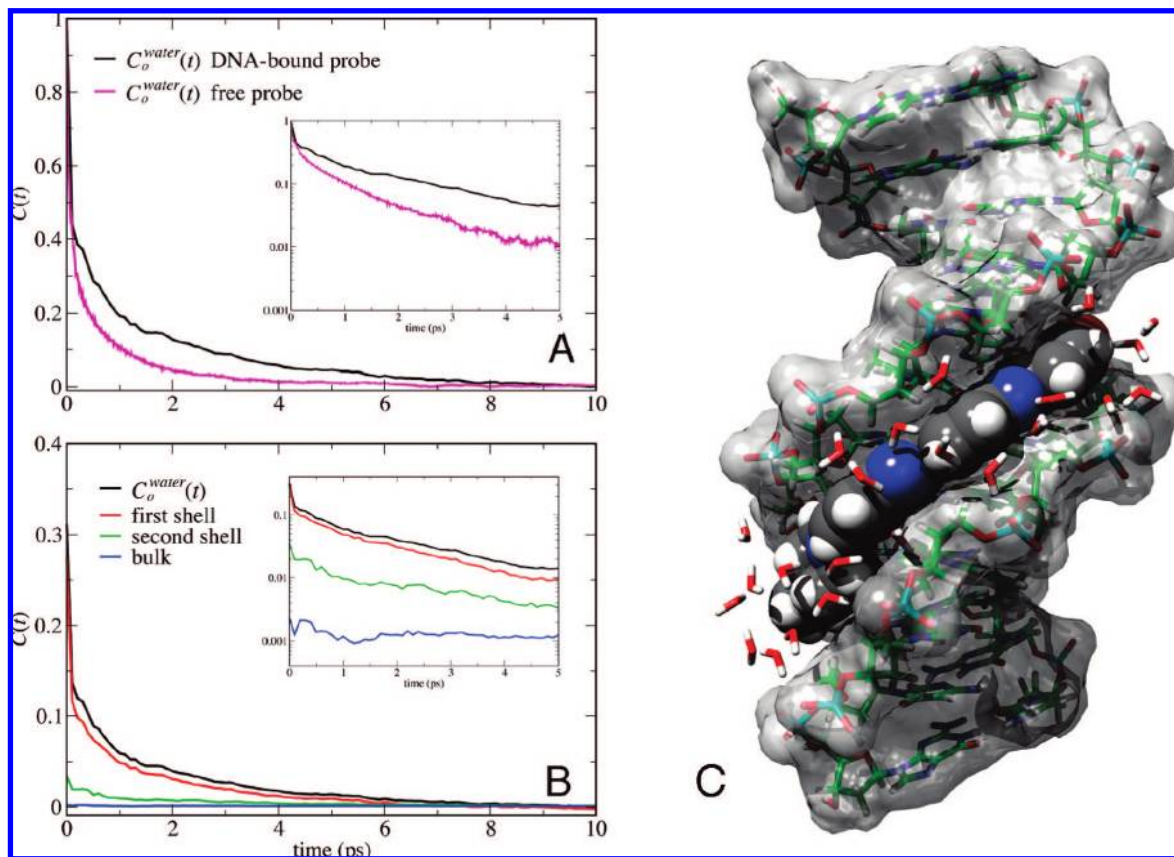


**Figure 4.** The water response. (A) Comparison of  $C_0^{\text{water}}(t)$  for the probe bound to DNA (black) and free in aqueous solution (magenta). Both partial correlation functions were normalized to 1.0 to facilitate direct comparison. The water response is similar for both environments, slowing by a factor of 2–3 when the probe is bound to DNA (also Table 2). (B) Spatial decomposition of  $C_0^{\text{water}}(t)$  for the DNA-bound probe into contributions from the first and second solvation shells of the probe (red and green, respectively) and bulk water (blue, defined as water beyond the second shell of the probe). (C) The first solvation shell in a typical simulation frame (average 26 waters).

simulations are capturing key differences in the bulk water and DNA/water interface environments. While the experimental solvation response is a collective property, we are able to decompose the total calculated response into contributions from the individual water, DNA, counterion, and solute conformational components to investigate the molecular origins of the observed time scales. Decomposition of  $C(t)$  using partial time correlation functions reveals that the water component decays rapidly, while the long-time constant ( $\tau_3$ ) and offset ( $a_4$ ) are associated almost exclusively with DNA motion (Figure 3). Decomposition of  $S(t)$  into individual response functions supports these findings (Supporting Information). While the contribution of ions tends to be prominent in auto- and cross-correlations, it is small in magnitude,  $<1\%$  for  $C^{\text{ion}}(t)$ , and negative in our partial correlations, as well as the  $S(t)$  decomposition. This suggests that while ion motion is strongly coupled to the other components, most lie outside of the probe range (small magnitude), and at least in our simulations, interact more favorably with the excited-state than the ground state (negative contribution). More detailed characterization of the ion behavior is beyond the scope of the current work.

To better document early events in the solvation response, the first 5 ps of the nonequilibrium simulations and the first 2 ns of each of the seven ground-state equilibrium simulations were collected at 10 fs resolution. At this 10-fold higher resolution, reproducible high frequency oscillations are clearly visible in both  $C(t)$  and  $S(t)$  for the probe free in solution and bound to DNA (Figure 2, inset). The origin of these oscillations

was previously traced to the conformational flexibility of the probe itself and the direct inclusion of solute intramolecular potential in the instantaneous solvation energy,  $\Delta E(t)$ .<sup>29</sup> The oscillations in  $C^{\text{conf}}(t)$  for the DNA-bound probe have similar frequencies, but larger amplitude, and take substantially longer to decorrelate. Fourier transforms suggest that this is due to coupling between DNA and H33258 motion (Supporting Information).

**C. Water Contribution.** While the characteristic time scales for the collective solvation response,  $C(t)$ , increase by a full order of magnitude when the probe is bound to DNA (Table 1), the time scales for the isolated water component,  $C^{\text{water}}(t)$ , only increase by a factor of 2–3 (Table 2, part A of Figure 4). Further analysis clarifies this finding, revealing that  $C^{\text{water}}(t)$  is dominated by the water molecules that comprise the first solvation shell of the probe (part B of Figure 4). The response of the second solvation shell is small but significant, and there is virtually no contribution from water molecules beyond the second shell of the probe. Therefore,  $C^{\text{water}}(t)$  primarily describes the motion of a relatively mobile group of waters that solvate the DNA sugar–phosphate backbone and the probe itself (part C of Figure 4). The bound probe has displaced the most motionally restricted water molecules of the minor groove, and the major groove waters are too distant to make a substantial contribution. As a result, water solvating H33258 bound to DNA does not behave dramatically differently from water solvating the unbound probe. This finding contradicts the original interpretation of the DNA/H33258 Stokes shift experiments,<sup>12</sup>

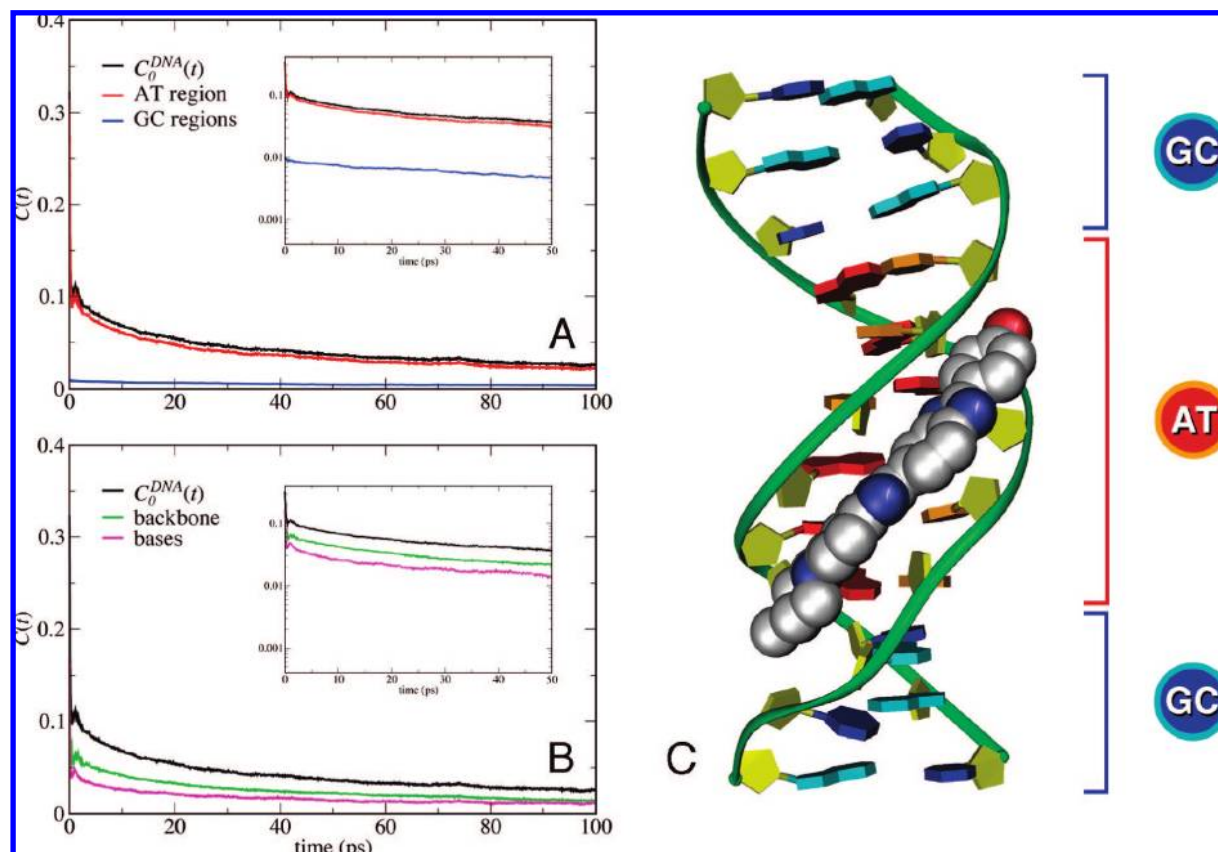


**Figure 5.** The DNA response. Spatial decomposition of  $C_0^{DNA}(t)$  (black) into contributions from (A) the central A·T region (red) and terminal G·C regions (blue), and (B) the bases (magenta) and sugar–phosphate backbone (green). All of the DNA subcomponents contribute to the long-time decay. The structure of the DNA/H33258 complex is shown in panel (C), with A (red), T (orange), G (cyan), C (blue), and the backbone (green/yellow).

but is consistent with MRD experiments in proteins.<sup>15,16</sup> The latter have shown that the vast majority of water molecules that hydrate proteins exhibit an average rotational retardation factor of  $\sim 2$  compared to bulk water, increasing to  $\sim 5$  when the most strongly motionally restricted water molecules are included.<sup>16</sup> Our findings are also remarkably consistent with recent spectroscopic studies of aqueous NaBr solutions in which the water hydrogen-bond rearrangement dynamics slowed by a factor of 3 (at most) relative to bulk water, even for the most concentrated solutions.<sup>36</sup>

Our results also agree with Nilsson and Halle's solvation dynamics calculations in proteins<sup>9</sup> but disagree with the findings of Hynes and co-workers who used the nucleotide bases themselves as intrinsic probes of solvation dynamics in DNA simulations.<sup>10</sup> On the basis of auto- and cross-correlations of  $C(t)$ , they attributed the slow decay to the water and ion components, not DNA. Berg and co-workers also associated long reorganization times with water based on autocorrelations calculated using a novel polarization model for decomposition.<sup>6</sup> Autocorrelation of  $\Delta E^{\text{water}}(t)$  also exhibits a long-time tail similar to the Hynes results; however, the components of the dynamic Stokes shift are rigorously related to partial correlation functions (eq 4), not autocorrelations. This is demonstrated empirically by the disagreement between our component autocorrelations and the  $S(t)$  decomposition (Supporting Information, Figure S-1). Nilsson and Halle have suggested that the long-time tails

commonly seen in water autocorrelations reflect dynamic coupling of collective water motion with slow biomolecule motion, not slow motion of individual water molecules.<sup>9</sup>

Unlike Hynes and co-workers, we also find a long-time tail for the autocorrelation of  $\Delta E^{\text{DNA}}(t)$ , as well as significant DNA cross-correlations. So, while the difference in decomposition method appears to be the primary source of the discrepancies in our findings, there may be real physical differences as well. Interestingly, the sensitivity of solvation dynamics experiments to local probe–environment interactions<sup>7,37–39</sup> suggests that the nature and position of the probe itself (fluorescent minor-groove binder vs intrinsic DNA base) could also contribute to the discrepancy. We are likely describing a different subset of water molecules at the DNA interface than those of the simulations using probes centered on the DNA bases.<sup>6,10</sup> This would be consistent with studies in proteins, which have demonstrated that the relative contributions of water and protein to the long-time solvation response can vary by location and even reverse with conformational changes.<sup>7,8</sup> In the H33258/DNA system, the water molecules important to the solvation response are not, in fact, confined because the probe itself has displaced water from the minor groove. Recent studies from the Fayer laboratory confirm that the reorientation dynamics of water are much more sensitive to the effects of confinement than to specific interfacial

(36) Park, S.; Fayer, M. D. *Proc. Natl. Acad. Sci. USA* **2007**, *104*, 16731–16738.

(37) Lesch, H.; Schlichter, J.; Friedrich, J.; Vanderkooi, J. M. *Biophys. J.* **2004**, *86*, 467–472.

(38) Muino, P. L.; Callis, P. R. *J. Chem. Phys.* **1994**, *100*, 4093–4109.

(39) Maroncelli, M.; Fleming, G. R. *J. Chem. Phys.* **1988**, *89*, 5044–5069.

interactions.<sup>40</sup> It appears that multiple different probe locations are needed to investigate all of the local environments in DNA as well.

**D. DNA Contribution.** While the water component of the solvation response reflects the dynamics of a homogeneous mixture of small molecules, the DNA response describes the movement of a heterogeneous network of covalently bonded atoms. The two components exhibit different dynamics — while  $C^{\text{water}}(t)$  decays fully within 10 ps,  $C^{\text{DNA}}(t)$  exhibits slower decay and is primarily responsible for the longer time scales of the collective response (Figure 3).  $C^{\text{DNA}}(t)$  also exhibits a small recurrence in correlation at around 1 ps. This feature is also evident in  $S^{\text{DNA}}(t)$  and partial correlation functions,  $C^{\text{DNA}}(t)$ , computed at 10-fold higher temporal resolution (10 fs), as well as autocorrelations of  $\Delta E^{\text{DNA}}(t)$ . Such a recurrence has not been reported for proteins, nor in previous computational solvation dynamics studies in DNA that utilized probes based on the DNA bases themselves.<sup>6,10</sup> By contrast, in this work we simulate excitation of a noncovalently bound fluorescent probe. It is reasonable to suggest that the motion of DNA would be experienced in subtly different ways by a minor-groove binding probe compared to an integral probe that is part of the DNA structure. We are currently investigating this unique recurrence further in simulations of an integral fluorescent probe that replaces a DNA base.

In an effort to understand the microscopic origin of the DNA response, we decomposed  $\Delta E^{\text{DNA}}$  spatially into contributions from the central A•T segment of the dodecamer, d(CG-CAAATTTGCG), and the G•C ends (part A of Figure 5). The six base pair central A-tract, which forms the binding site for the probe, is primarily responsible for the shape and magnitude of the DNA response. The bordering G•C segments make a minor contribution to the long time scale and offset (~14%). We also decomposed  $\Delta E^{\text{DNA}}(t)$  into contributions from the base pairs and the negatively charged sugar–phosphate backbone that connects them. The backbone and base pairs are different chemically, but contribute nearly equally to the relaxation profile, including the long-time behavior (part B of Figure 5). Finally, we decomposed the response using an atom-based cutoff to divide the DNA into shells as well as decomposing by element (data not shown). Regardless of the method of decomposition, the long time scale and offset could not be

attributed to a single substructure of DNA, but instead appear to arise from motions that encompass the entire dodecamer.

#### IV. Summary and Conclusions

According to time-resolved Stokes shift experiments, the collective solvation response to excitation of the fluorescent probe H33258 slows by an order of magnitude when the probe is bound to DNA, exhibiting at least two characteristic time scales, ~1.5 ps and ~20 ps.<sup>12</sup> There is conflicting evidence as to the microscopic origin of the slower time scale — some describe substantial retardation of water motion at biological interfaces, while others describe rapid water dynamics in the hydration layer with a slower biomolecular response. The equilibrium and nonequilibrium solvation dynamics calculations presented here for the minor-groove binding probe H33258 clearly associate the longer of the two collective time scales exclusively with DNA motion. This is consistent with the idea that solvation in complex environments includes the motion of components other than water.<sup>11,16</sup> In the present study, DNA effectively “solvates” the probe along with water and ions, and exhibits a distinct time dependence of reorganization. The water response to the DNA-bound probe is dominated by relatively mobile waters that surround the probe itself and neighboring regions of the DNA backbone and is not dramatically different from the response to the probe in solution, slowing by a factor of 2–3.

**Acknowledgment.** The authors gratefully acknowledge the Northwest Indiana Computational Grid (NWICG) and the Center for Research Computing (CRC) at the University of Notre Dame for financial support. Figures 1 and 5 were produced with *DINO*, Figure 4 and TOC graphic using *Chimera* package (supported by NIH P41 RR-01081).<sup>42</sup>

**Supporting Information Available:** Simulation details and plots of  $C_1(t)$ ,  $S(t)$ , Fourier transforms of  $C_0^{\text{DNA}}(t)$  and  $C_0^{\text{conf}}(t)$ , and complete ref 32. This material is available free of charge via the Internet at <http://pubs.acs.org>.

JA803728G

(40) Moilanen, D. E.; Levinger, N. E.; Spry, D. B.; Fayer, M. D. *J. Am. Chem. Soc.* **2007**, *129*, 14311–14318.

(41) Philippsen, A. *DINO: Visualizing Structural Biology*; <http://www.dino3d.org>, 2002.

(42) Pettersen, E. F.; Goddard, T. D.; Huang, C. C.; Couch, G. S.; Greenblatt, D. M.; Meng, E. C.; Ferrin, T. E. *J. Comput. Chem.* **2004**, *25*, 1605–1612.